Electronic Supplementary Material (ESI) for Dalton Transactions.

Supporting Information

Ensemble Effects on Allylic Oxidation within Explicit Solvation Environments

Hung M. Le,[1] Mariano Guagliardo,[2] Anne E. V. Gorden,[2] and Aurora E. Clark[1, 3]

(1) *Department of Chemistry, Washington State University, Pullman, Washington 99164, United States*[a)]

(2) *Department of Chemistry and Biochemistry, Texas Tech University, Lubbock, Texas 79430, United States*

(3) *Pacific Northwest National Laboratory, Richland, Washington 99352, United States*[b)]

[a)] Electronic mail: hung.le2@wsu.edu

[b)] Electronic mail: auclark@wsu.edu

The following figures demonstrate convergence of umbrella sampling for multiple reaction steps. In each reaction, we choose to perform WHAM with 150, 160, 170, 180, 190, and 200 equilibration steps (samples). In addition, we also show the overlapping of probability distribution of umbrella sampling bins for each reaction.

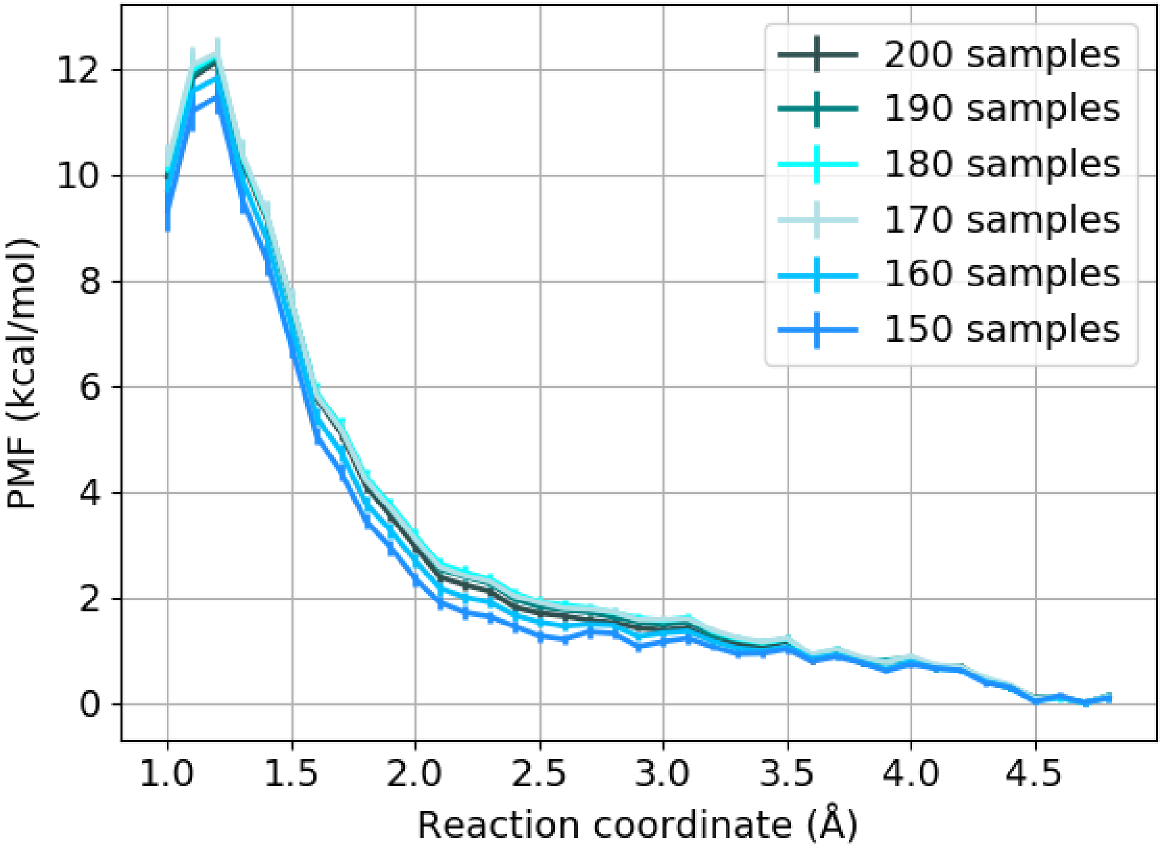

FIG. S1. PMF with various equilibration steps for the O(1)-H abstraction.

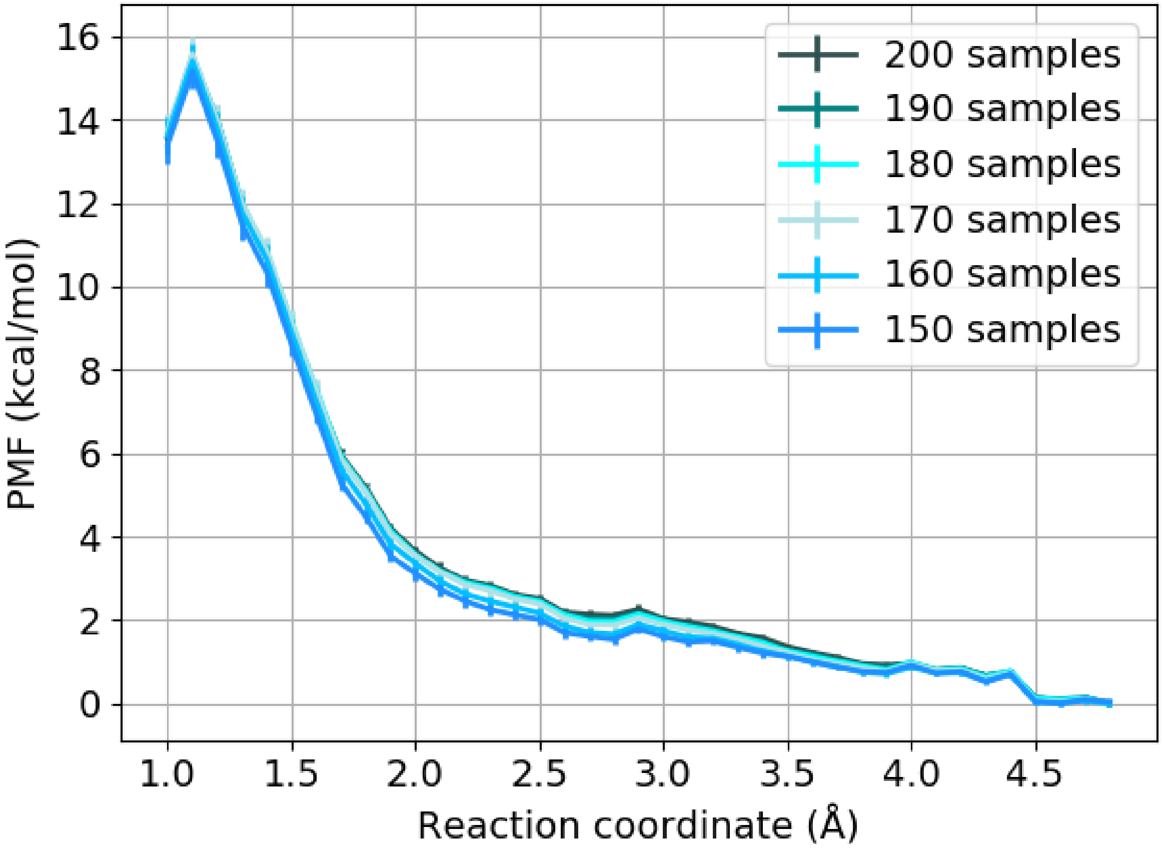

FIG. S2. PMF with various equilibration steps for the O(2)-H abstraction.

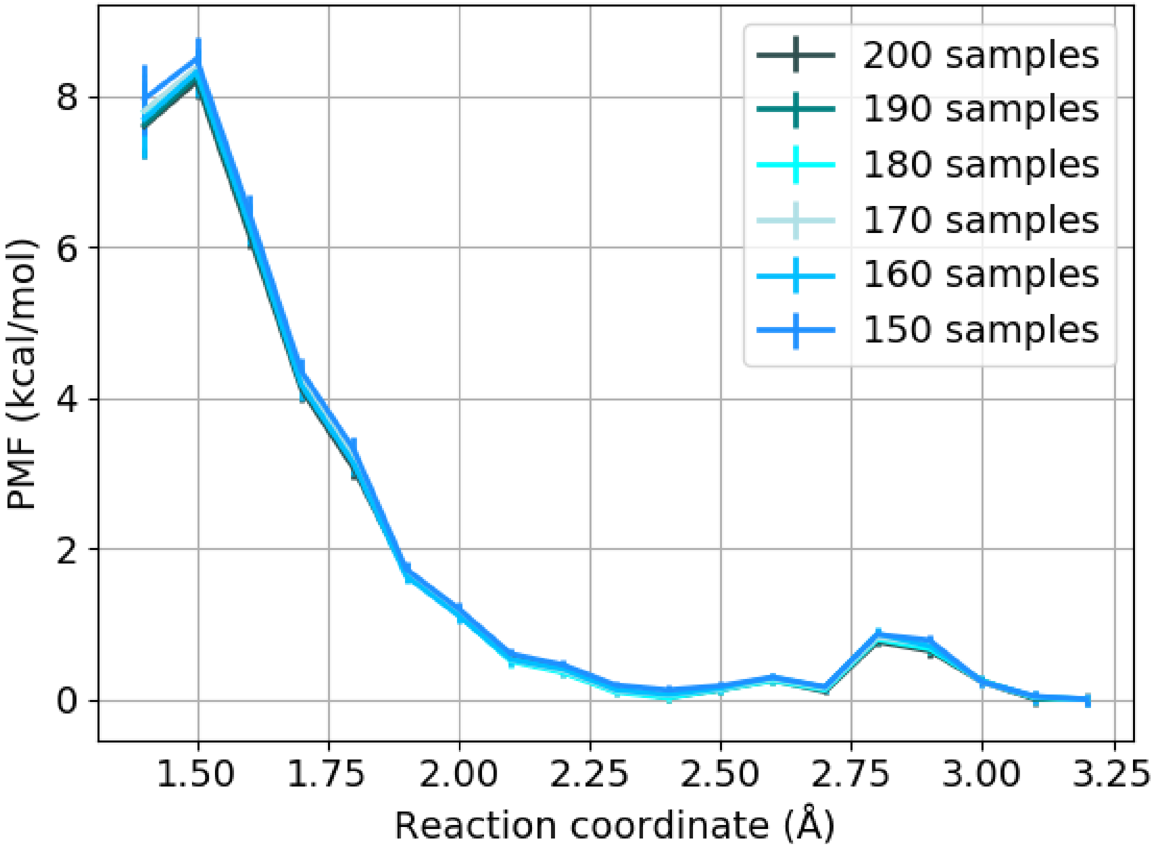

FIG. S3. PMF with various equilibration steps for the product formation (release of OH radical).

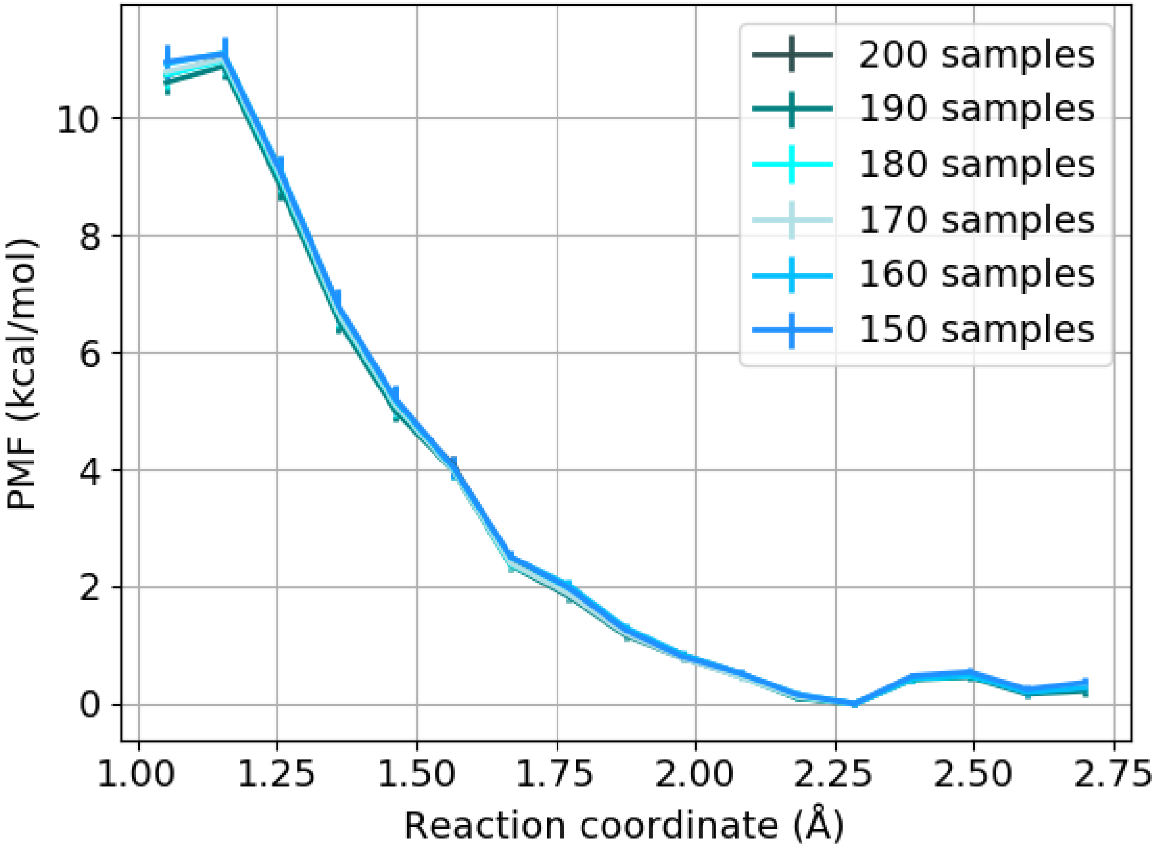

FIG. S4. PMF with various equilibration steps for the re-establishment of N-H bond.

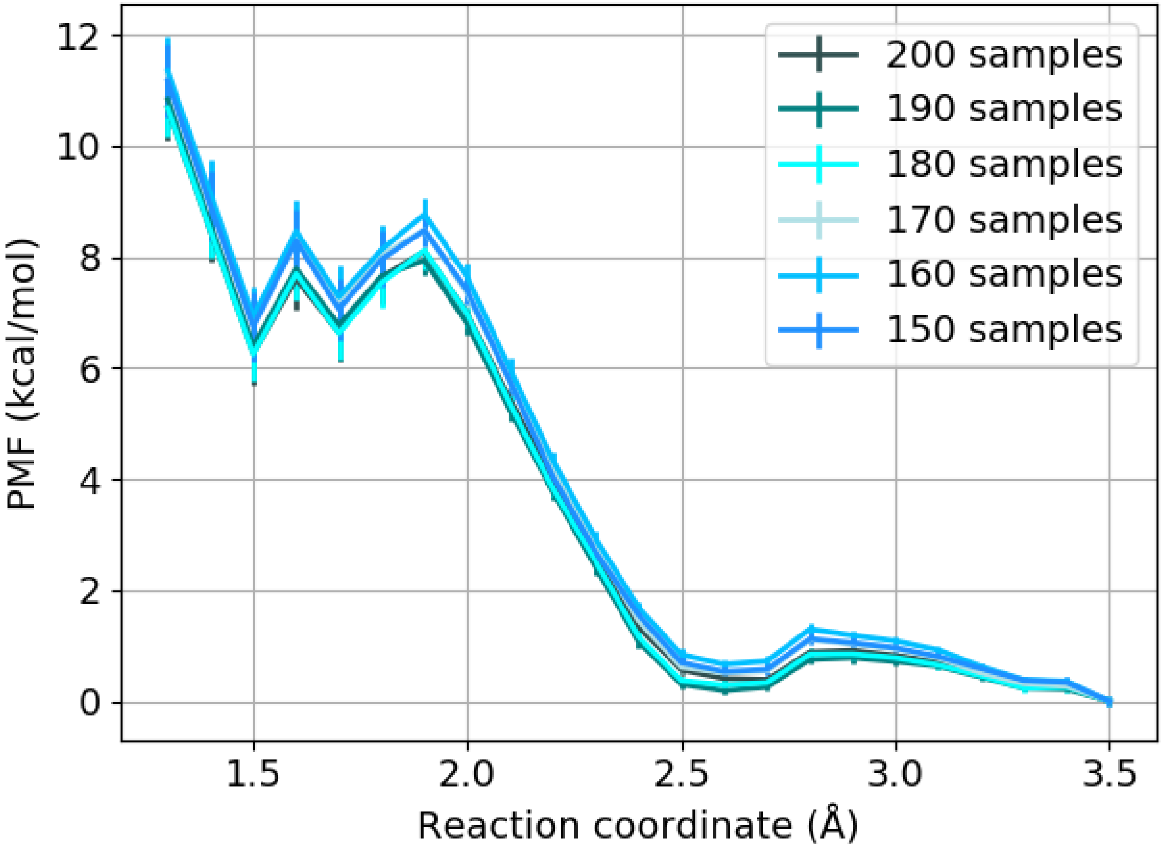

FIG. S5. PMF with various equilibration steps for the peroxide bond formation.

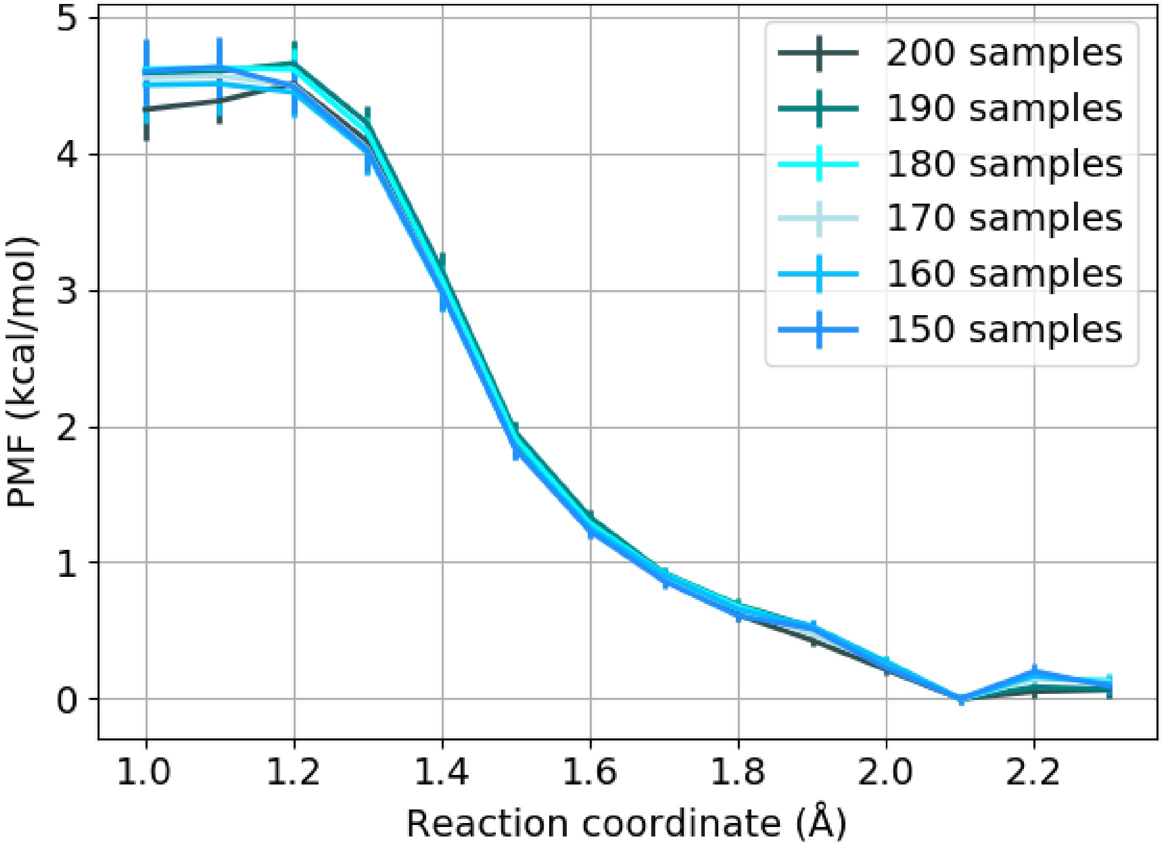

FIG. S6. PMF with various equilibration steps for the final step of catalyst recovery.

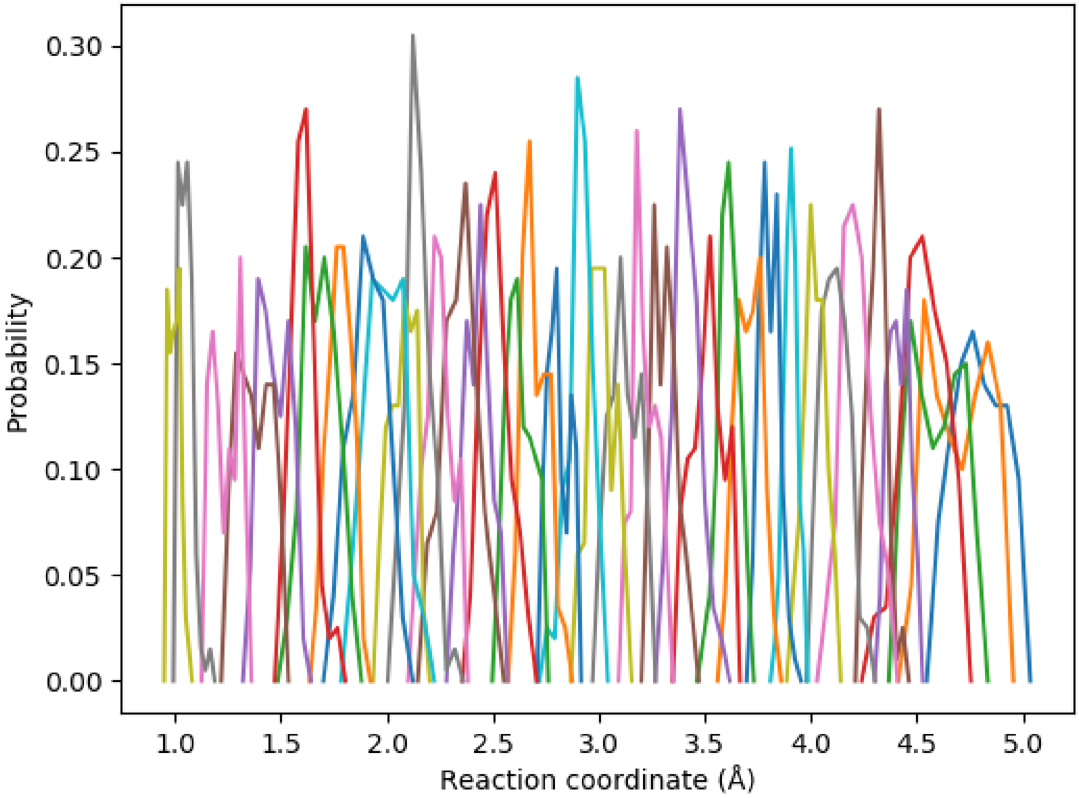

FIG. S7. Probability distribution showing overlapping of umbrella sampling bins along the reaction coordinate for O(1)-H abstraction.

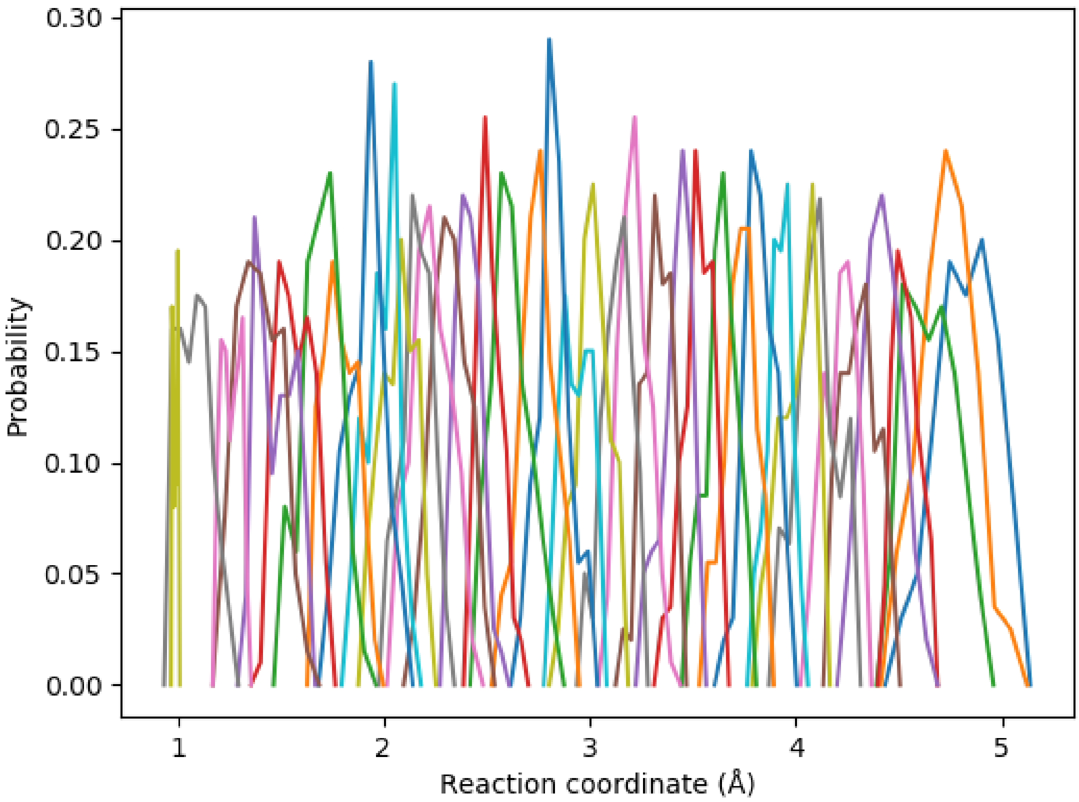

FIG. S8. Probability distribution showing overlapping of umbrella sampling bins along the reaction coordinate for O(2)-H abstraction.

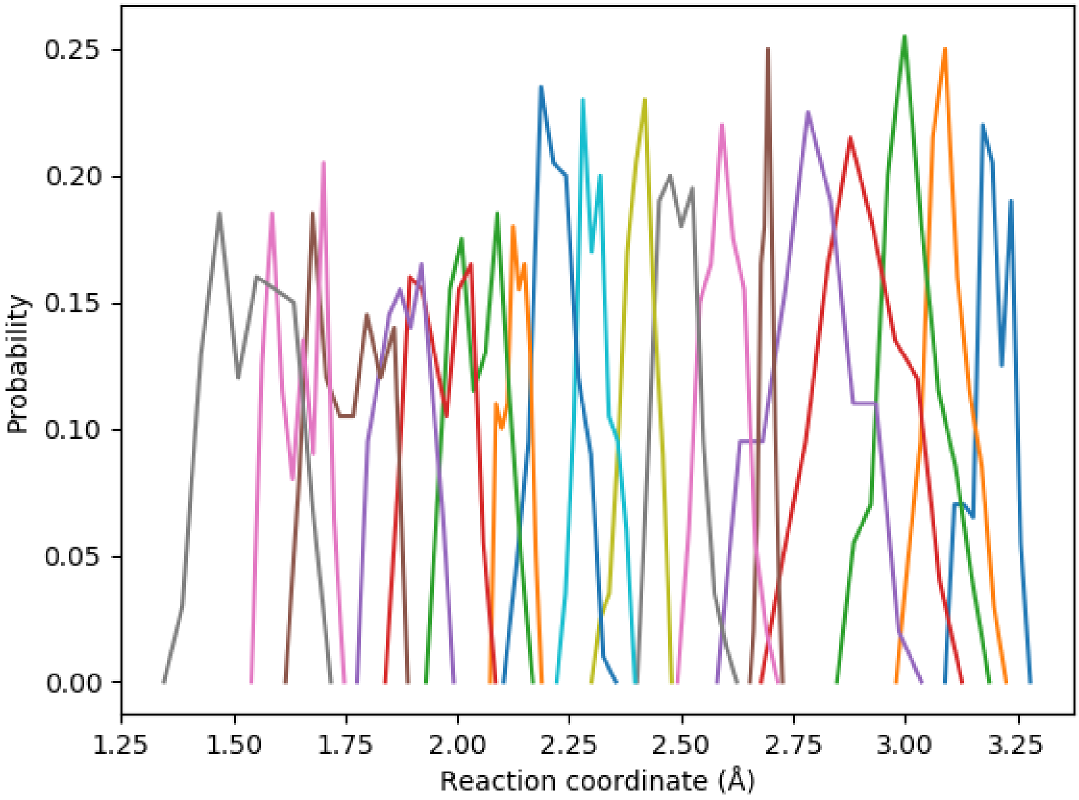

FIG. S9. Probability distribution showing overlapping of umbrella sampling bins along the reaction coordinate for the product formation (release of OH radical).

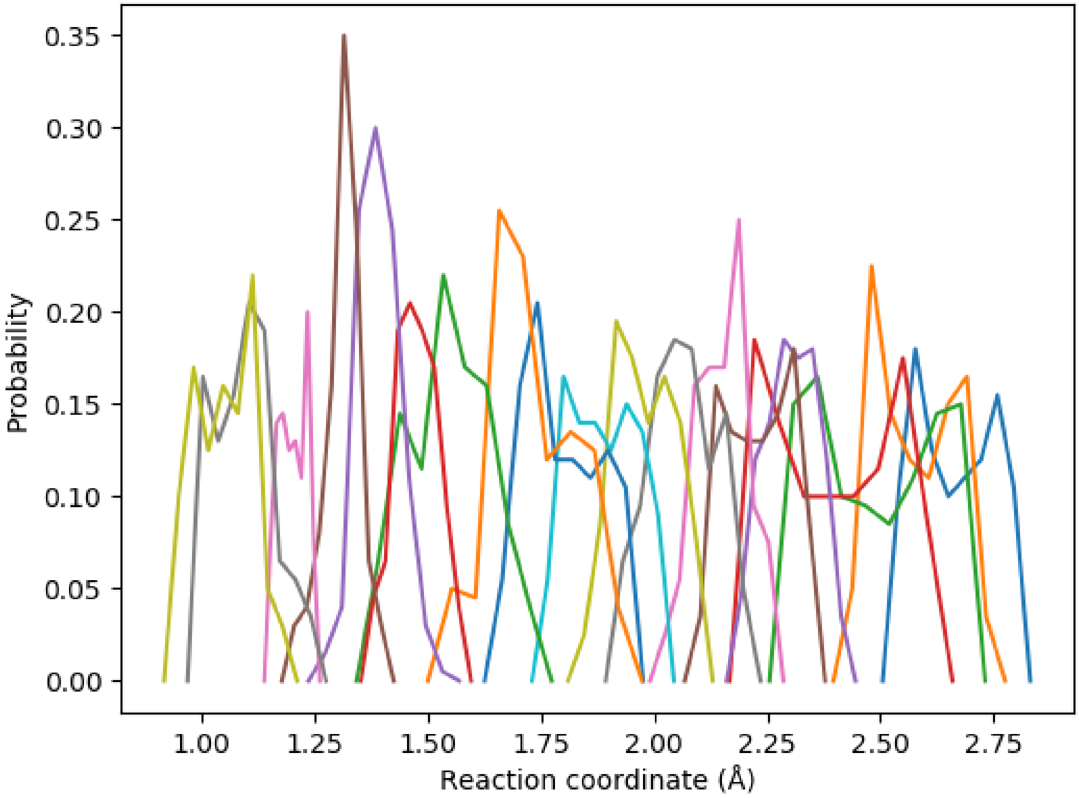

FIG. S10. Probability distribution showing overlapping of umbrella sampling bins along the reaction coordinate for the re-establishment of N-H bond.

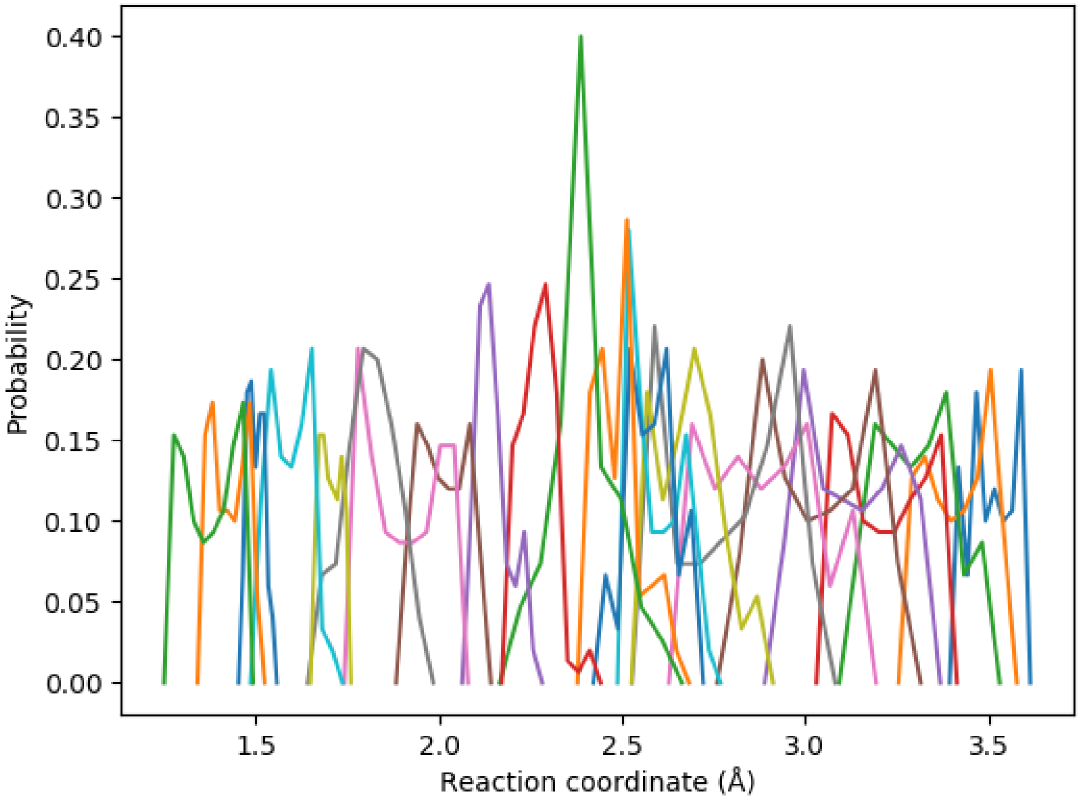

FIG. S11. Probability distribution showing overlapping of umbrella sampling bins along the reaction coordinate for the peroxide bond formation.

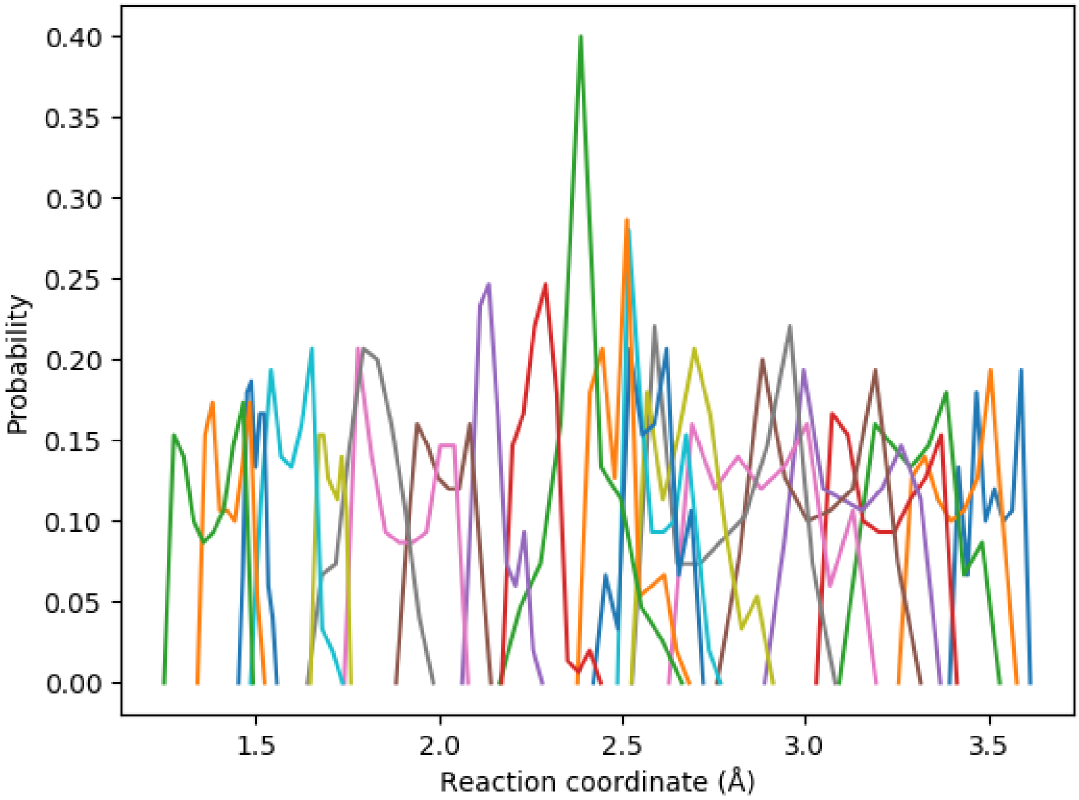

FIG. S12. Probability distribution showing overlapping of umbrella sampling bins along the reaction coordinate for the final step of catalyst recovery.

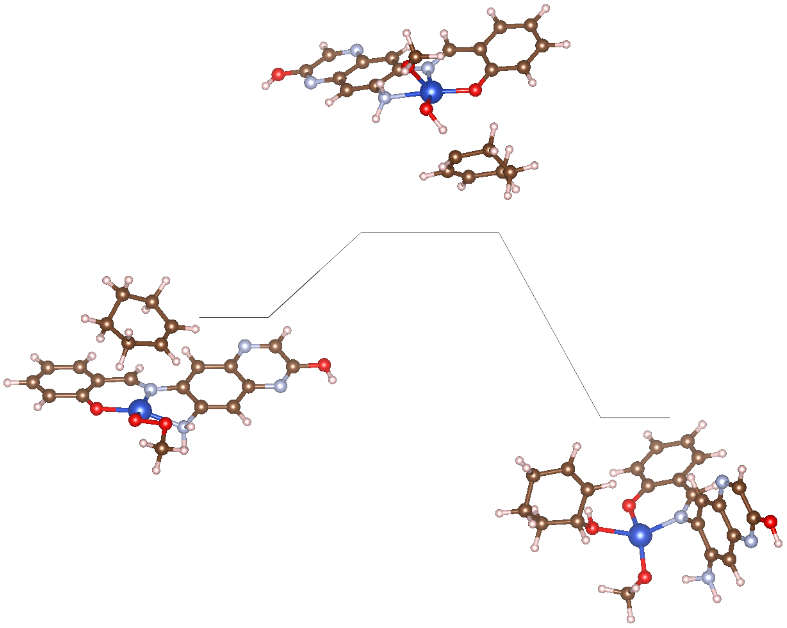

FIG. S13. O(1)-H abstraction given by static unrestricted B3LYP/6-31G(d) and B3LPY/6-31G(d) calculations with the consideration of acetonitrile media. There is one imaginary vibrational mode in the transition state.

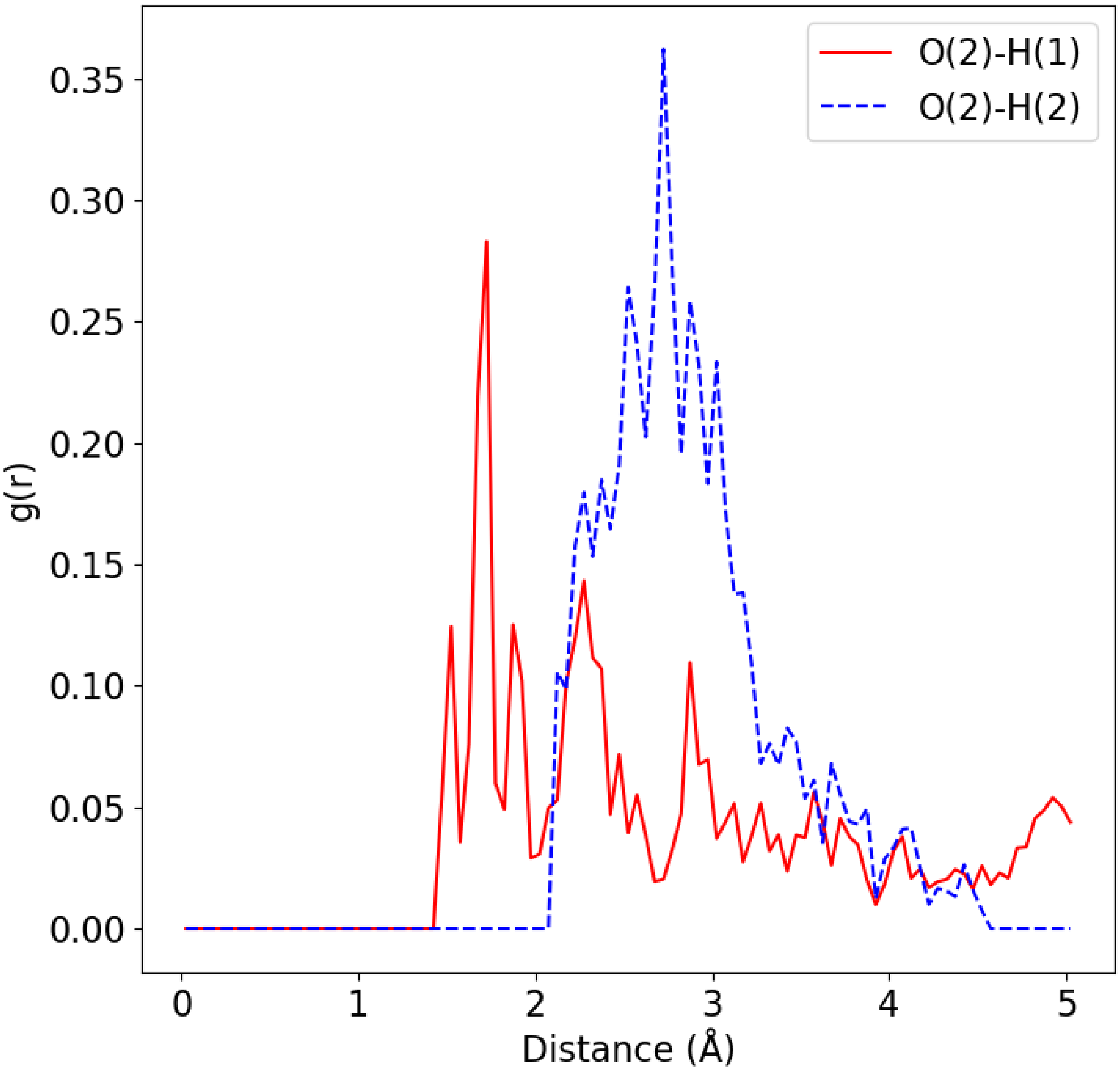

FIG. S14. Normalized radial distribution function of the O(2)...H(1) and O(2)...H(2) atom pairs in intermediate **INT-1** in the equilibration trajectory (1 ps).

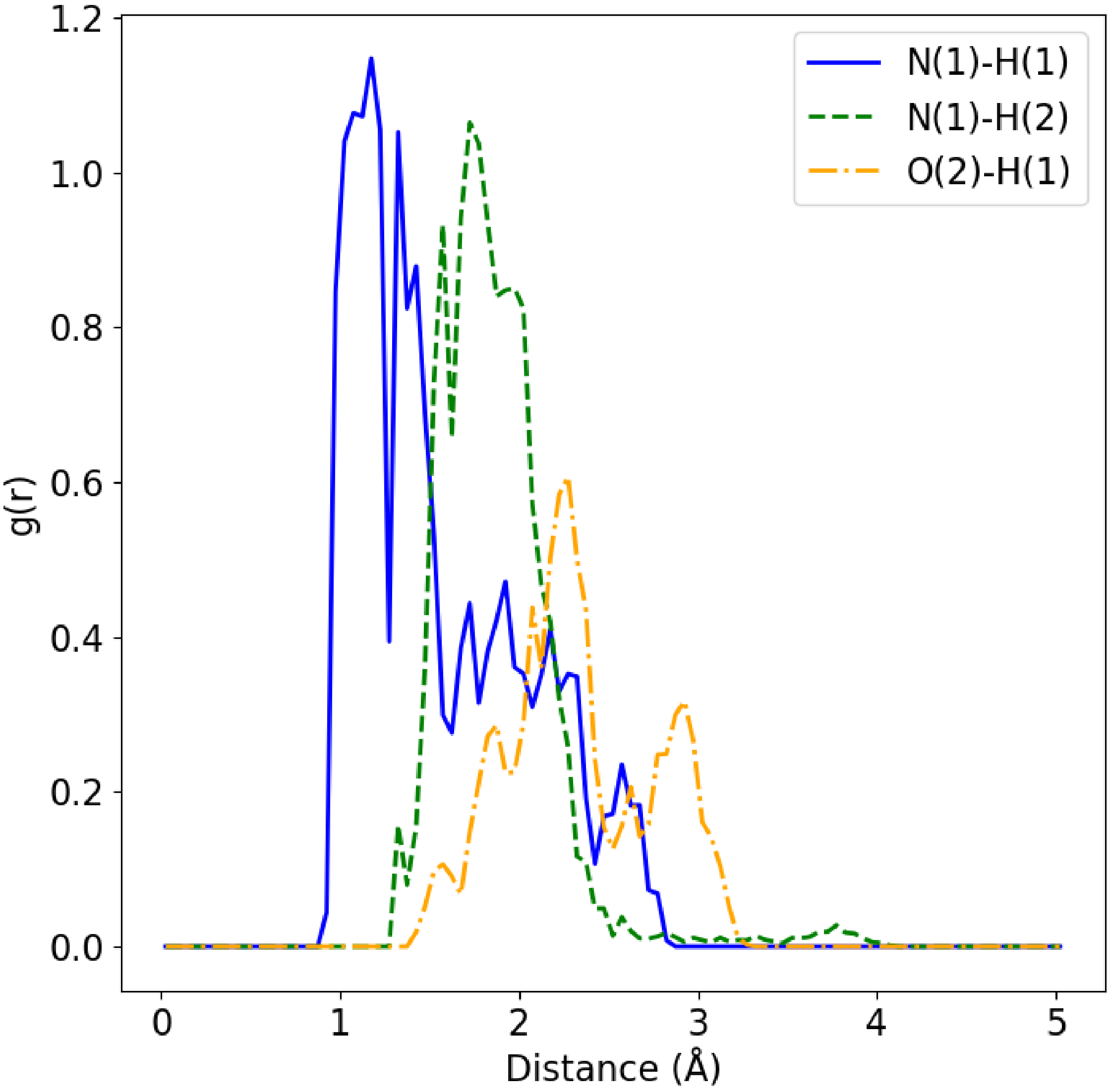

FIG. S15. Normalized radial distribution function of the N(1)...H(2) and O(2)...H(1) atom pairs in intermediate **INT-2** in the equilibration trajectory (1 ps) for N(1)-H(1) bond formation (recovery of catalyst).

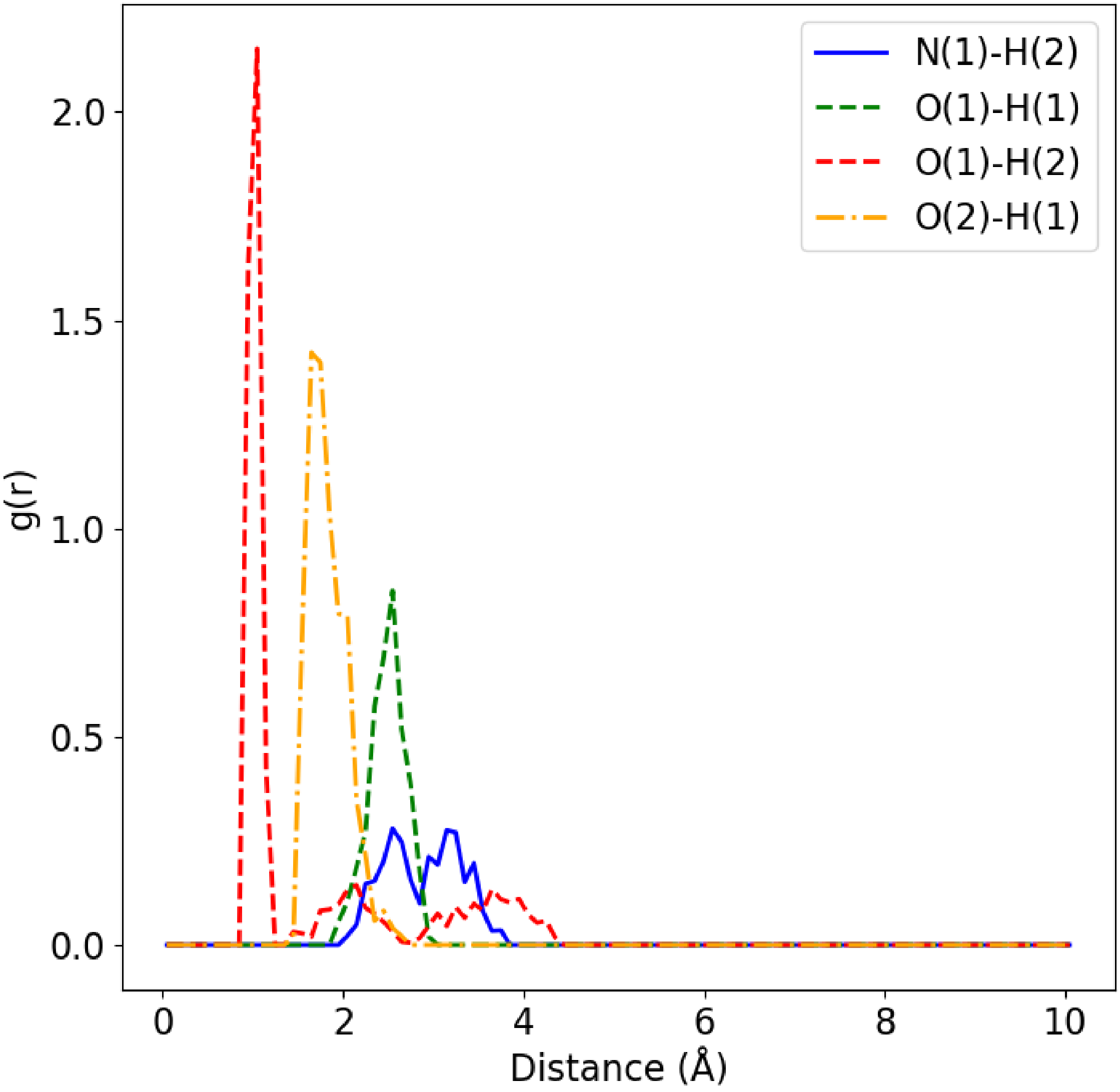

FIG. S16. Normalized radial distribution function of the O(2)...H(1) atom pair in intermediate **INT-3** in the equilibration trajectory (1 ps) for O(1)-O(2) bond formation (recovery of catalyst).

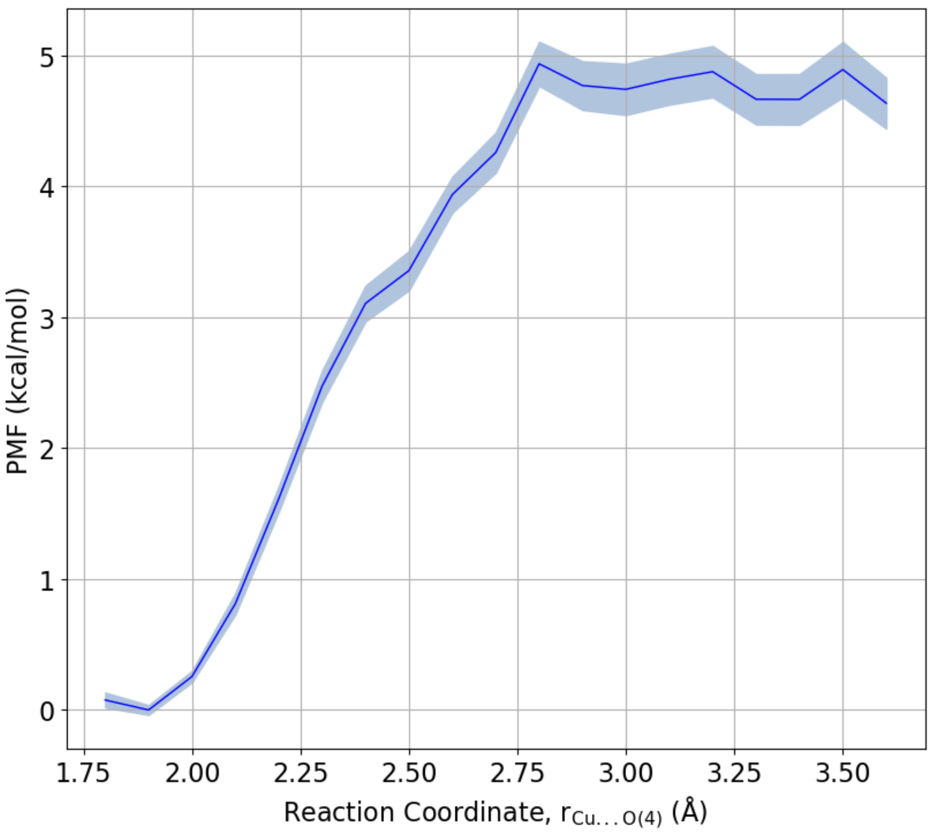

FIG. S17. PMF of the ·OOR residue attachment to the Cu site. The significant drop of free energy at 2.7 Å shows the strong attraction of the Cu-O(4) atom pair.

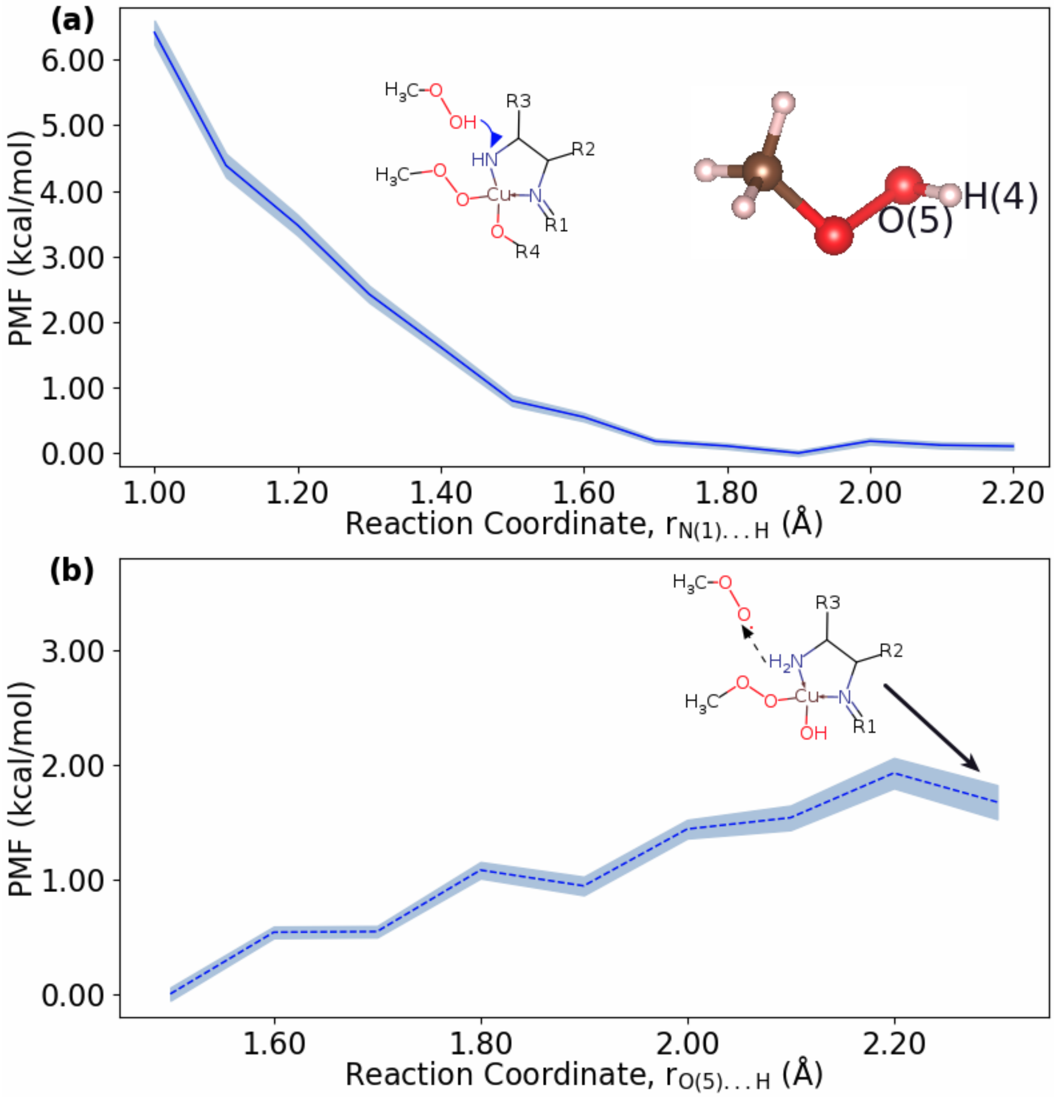

FIG. S18. (a) PMF of the N(1)-H(4) bond formation, (b) PMF of the O(5)...H(4) dissociation.

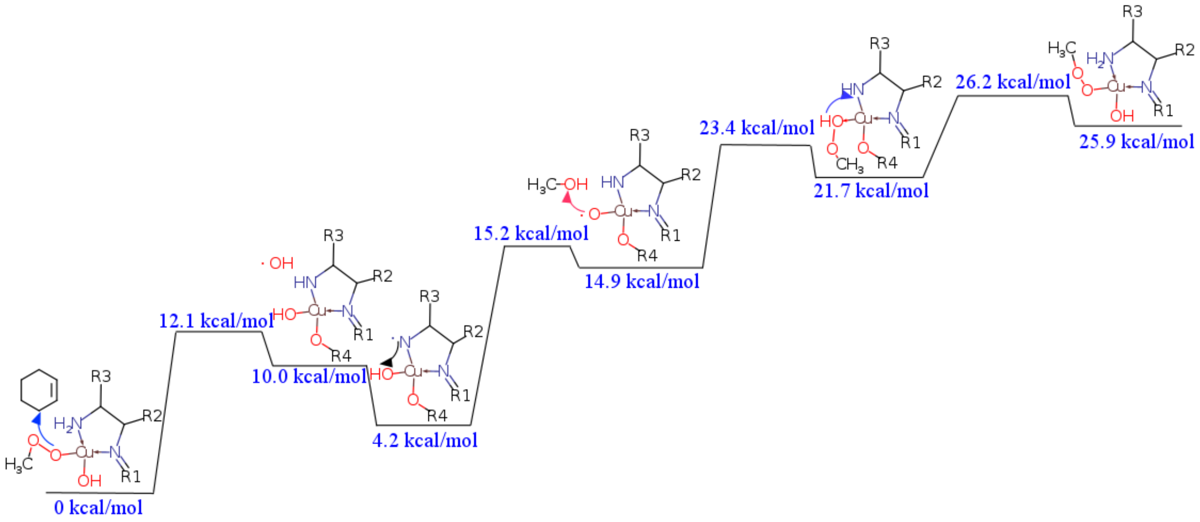

FIG. S19. The energetic span of the catalyst recovery process in the closed cycle. The step converting **INT-1** to **INT-2** is approximated using total electronic energy of **INT-1** before conversion and **INT-2** after conversion. The product formation step is omitted in this catalyst recovery cycle.

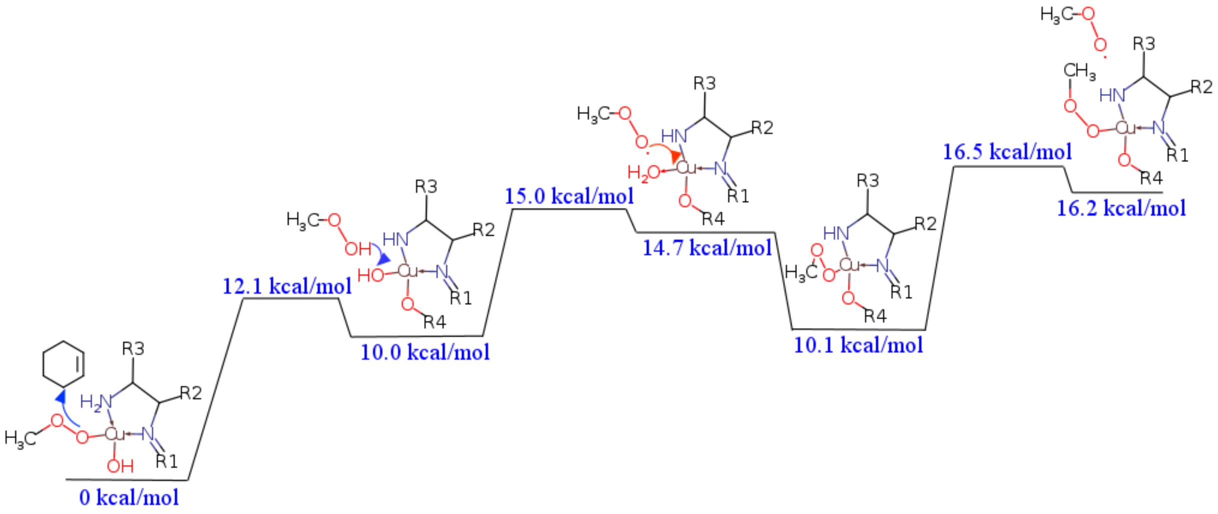

FIG. S20. The energetic span of the catalyst recovery process in the open cycle. The product formation step is omitted in this catalyst recovery cycle.